Is Hairpin Formation in Single-Stranded Polynucleotide Diffusion-Controlled?

ARTICLE *in* THE JOURNAL OF PHYSICAL CHEMISTRY B · AUGUST 2005

Impact Factor: 3.3 · DOI: 10.1021/jp044838a · Source: PubMed

2 AUTHORS:

Anjum Ansari
University of Illinois at Chicago
53 PUBLICATIONS **3,093** CITATIONS
SEE PROFILE

Serguei Kuznetsov
University of Illinois at Chicago
40 PUBLICATIONS **673** CITATIONS
SEE PROFILE

Is Hairpin Formation in Single-Stranded Polynucleotide Diffusion-Controlled?

Anjum Ansari*,†,‡ and Serguei V. Kuznetsov†

Department of Physics and Department of Bioengineering, University of Illinois at Chicago, 845 West Taylor Street, Chicago, Illinois 60607

Received: November 10, 2004; In Final Form: February 12, 2005

An intriguing puzzle in biopolymer science is the observation that single-stranded DNA and RNA oligomers form hairpin structures on time scales of tens of microseconds, considerably slower than the estimated time for loop formation for a semiflexible polymer of similar length. To address the origin of the slow kinetics and to determine whether hairpin dynamics are diffusion-controlled, the effect of solvent viscosity (η) on hairpin kinetics was investigated using laser temperature-jump techniques. The viscosity was varied by addition of glycerol, which significantly destabilizes hairpins. A previous study on the viscosity dependence of hairpin dynamics (Wallace et al. *Proc. Natl. Acad. Sci. U.S.A.* **2000**, *98*, 5584), in which all the changes in the measured rates were attributed to a change in solvent viscosity, reported an apparent scaling of relaxation times (τ_r) on η as $\tau_r \sim \eta^{0.8}$. In this study, we demonstrate that if the effect of viscosity on the measured rates is not deconvoluted from the inevitable effect of change in stability, then separation of τ_r into opening (τ_o) and closing (τ_c) times yields erroneous behavior, with different values (and opposite signs) of the apparent scaling exponents, $\tau_o \sim \eta^{-0.4}$ and $\tau_c \sim \eta^{1.5}$. Under isostability conditions, obtained by varying the temperature to compensate for the destabilizing effect of glycerol, both τ_o and τ_c scale as $\sim\eta^{1.1\pm0.1}$. Thus, hairpin dynamics are strongly coupled to solvent viscosity, indicating that diffusion of the polynucleotide chain through the solvent is involved in the rate-determining step.

Introduction

Palindromic regions of single-stranded (ss) DNA and RNA can form secondary structures such as hairpins by base-pairing between neighboring self-complementary sequences. The formation of hairpin structures in ssDNA and their role in biological processes is well documented in both prokaryotic and eukaryotic systems.[1−3] Hairpin structures are also useful drug targets because their overall shape and geometry differ significantly from regular double-stranded (ds) DNA.[4,5] In RNA molecules, hairpins represent the dominant elements of secondary structure and serve as nucleation sites for the initiation of RNA folding.[6,7] Tertiary interactions of hairpin loops and bulges in RNA molecules regulate their diverse activities.[8−11] The discovery that RNA molecules can function as enzymes[12] has sparked a renewed interest in the problem of RNA folding.[13]

A major effort in basic biopolymer science is directed toward an understanding of the energetics and mechanisms by which DNA or RNA molecules form their secondary and higher-order structures. Kinetics measurements on secondary structure formation in ss polynucleotide provide insights into the conformational flexibility of these chains and the nature and strength of the intrachain interactions. In this connection, short oligomers that form hairpin structures in solution represent an ideal model system to investigate the interactions that stabilize secondary structure. In the case of RNA, in which the hairpins make up a significant part of its secondary structure, an understanding of the dynamics of how hairpins fold is a starting point for understanding the folding of larger RNA molecules.

Hairpin formation in self-complementary ss oligomers has long been recognized as consisting of two steps, "nucleation", which is the formation of a stable loop, followed by the "zipping" of base pairs to form the stem.[14] If intrachain interactions are ignored and the ss chain is treated like an ideal semiflexible polymer, then the purely entropic conformational search time for the two ends of the chain to come together is estimated to be tens of nanoseconds.[15,16] However, several measurements indicate that hairpins with small loops form on time scales of tens of microseconds.[17−20] An intriguing puzzle is the origin of this separation in time scales by approximately 3 orders of magnitude between the estimated end-to-end contact time for a semiflexible polymer and the observed times for hairpin formation, which raises a fundamental question: Why is hairpin formation so slow? That is, what is the rate-determining step?

One explanation for a similar separation in time scales, observed in the cyclization of λ DNA, which also occurs more than 3 orders of magnitude slower than the end-to-end contact time expected for dsDNA, was first proposed by Wang and Davidson.[21−23] They argued that DNA cyclization is reaction-controlled, i.e., the rate-determining step in the joining of the two cohesive ends of λ DNA is the very slow chemical step of base-pair formation and not the diffusion-controlled time for contact formation. They based their arguments on two observations: First, the temperature dependence of the measured cyclization times exhibited a very large (~24 kcal/mol) activation energy. Second, the viscosity dependence of the cyclization times did not follow a simple scaling with solvent viscosity as expected for a diffusion-controlled reaction. Hairpin closing times, however, are only weakly temperature-dependent in aqueous solution and, in fact, exhibit *negative* activation energies

* Author to whom correspondence should be addressed. Phone: (312) 996-8735. Fax: (312) 996-9016. E-mail: ansari@uic.edu.
† Department of Physics.
‡ Department of Bioengineering.

10.1021/jp044838a CCC: $30.25
Published on Web 06/09/2005

for the closing step.[16] The viscosity dependence of the opening and closing times is in question and is the main topic of this paper.

There has been, to our knowledge, only one detailed study, by Klenerman and co-workers,[24] of the effect of solvent viscosity on the dynamics of hairpin formation. The authors of this study monitored the conformational fluctuations of a ssDNA hairpin labeled with fluorescence donor and acceptor dyes at the ends and found that the relaxation times, obtained from the decay of a fluorescence correlation function, scaled with solvent viscosity as $\eta^{0.8}$. One of the major obstacles in interpreting the apparent viscosity dependence of the measured relaxation rates is that the addition of viscogenic cosolvents invariably affects the stability of hairpins and duplexes.[23,25] It is not straightforward to obtain the true viscosity dependence without first correcting for these inevitable changes in stability. Klenerman and co-workers reached an erroneous conclusion that all the changes in the observed rates upon addition of glycerol could be attributed to changes in the solvent viscosity.

One approach to investigate the effect of solvent viscosity on relaxation rates is to make measurements under isostability conditions, e.g., compensating for the changes in stability upon addition of viscogenic cosolvents by varying some other parameter that also affects the stability. This approach has been applied in studies of the viscosity dependence of protein folding kinetics.[26−28] In this paper, we investigate the changes in the stability of hairpins in solvents with varying glycerol concentrations and establish isostability conditions for which the viscosity dependence can be isolated. Under these conditions, we find that the opening and closing times scale nearly linearly with the solvent viscosity. These results, together with the weak temperature dependence of the hairpin formation step, support the notion that the slow kinetics of hairpin formation is not from a reaction-controlled process but may be the result of slow configurational diffusion of the chain, as a result of significant intrachain interactions prior to the nucleation step.[20,29]

Methods

Materials. The DNA oligomer in this study is 5′-CGGATAA-(T_8)TTATCCG-3′, denoted as hairpin H. The central T_8 sequence of the oligomer forms a loop with seven base pairs in the stem of the hairpin. The oligomer was purchased from Oligos Etc. (Wilsonville, OR). All samples were HPLC purified. The buffer solution was 10 mM sodium phosphate, pH 7.5, 100 mM NaCl (or 1 M NaCl) and 0.1 mM EDTA. Glycerol−buffer mixtures were prepared gravimetrically. The final concentrations of DNA oligomers in the samples were ∼30 μM for equilibrium melting measurements and ∼80 μM for the kinetics measurements. The glycerol concentrations were 0%, 15%, 30%, 49%, and 73%, in 100 mM NaCl (49% and 74%, in 1 M NaCl) in the samples used for equilibrium measurements, and 0%, 15%, 30%, 47%, and 70%, in 100 mM NaCl (50% and 75%, in 1 M NaCl) in the samples used for kinetics measurements. The temperature-dependent viscosity of each of the glycerol samples was obtained by linear interpolation using the table of viscosity values compiled by Newman.[30]

Equilibrium Measurements. Optical melting profiles were obtained by measuring changes in the absorbance at 266 nm as a function of temperature, using a Hewlett-Packard 8452 (Palo Alto, CA) diode array single beam spectrophotometer equipped with a temperature controller. The absorbance profiles were typically averaged for approximately six cycles of heating and cooling. The melting profiles for the forward and reverse melts were identical to within the error in these measurements, and there was no signature of duplex formation under the conditions of our measurements, as established by the concentration dependence of the melting profiles.

The absorbance versus temperature profiles were normalized to obtain the fraction of molecules in the unfolded (or open) state, $f_U(T)$, by fitting the absorbance profiles $A(T)$ to a two-state transition plus an upper (A_U) and a lower (A_L) baseline: $A(T) = f_U(T)[A_U(T) - A_L(T)] + A_L(T)$. The upper and lower baselines were parametrized as straight lines with independently varying slopes. $f_U(T)$ was described in terms of a van't Hoff expression

$$f_U(T) = \frac{1}{1 + \exp\left[-\frac{\Delta H}{R}\left(\frac{1}{T} - \frac{1}{T_m}\right)\right]} \quad (1)$$

Here, ΔH is the enthalpy of a fully intact hairpin relative to the unfolded state and is assumed to be temperature-independent. T_m is the melting temperature of the hairpin at which $f_U = {}^1/_2$. Equation 1 assumes that the unfolding transition occurs without any significant changes in the heat capacity of the system. For a more accurate parametrization of the melting transition, the heat capacity changes should be explicitly included.[31,32]

Laser Temperature-Jump Spectrometer. The relaxation kinetics were monitored by measuring the change in absorbance as a function of time after a laser temperature jump (T-jump). The T-jump spectrometer is described in detail elsewhere.[15,20] Briefly, a 6-ns pulse at 1.06 μm from a Nd:YAG laser (Continuum Surelite II) is used to pump a 2-m-long Raman cell consisting of high-pressure methane gas. The first Stokes line at 1.54 μm is separated from other wavelengths by a Pellin-Broca prism and focused down to about 1 mm (full width at half-maximum) on one side of the sample cuvette. A typical T-jump achieved with this setup is about 10 °C in a cuvette with path length ∼300 μm. The probe source is a Xe/Hg 200-W lamp with an interference filter at 265 nm. The light from the lamp is focused onto an ∼300-μm aperture, which is imaged onto the sample cuvette in the center of the heated volume. The transmitted intensities are detected by a photomultiplier tube and digitized using a 500-MHz transient digitizer (HP 54825A).

The transmitted intensities $I(t)$ were converted into absorbance changes, $\Delta OD(t) = -\log(I(t)/I_0)$ where I_0 is the average intensity prior to the T-jump. The observed kinetics were single-exponential under the conditions of our experiments and were fit to the following function

$$\Delta OD(t) = \Delta A[1 - \exp(-k_r t)] + \delta A \quad (2)$$

Here, ΔA is the total change in absorbance, as a result of the unwinding of the hairpin, k_r is the relaxation rate, and δA is the amplitude of a rapid change in the absorbance of the sample within the time resolution of the T-jump spectrometer. δA has contributions from an apparent change in the optical density of the sample from thermal lensing effects[33] and from any unresolved relaxations. The initial temperature of the sample T_i was measured using a thermistor (YSI 44008, YSI, Yellow Springs, OH) that was in direct contact with the sample holder. The final temperature T_f was determined by comparing the measured change in absorbance ΔA with the equilibrium absorbance versus temperature melting profiles. The relaxation rates thus obtained at each final temperature are the sum of the opening and closing rates: $k_r = k_c + k_o$. The equilibrium constant obtained from the melting profiles, $K_{eq} = (1 - f_U)/f_U$, gives the ratio of the opening and closing rates: $K_{eq} = k_c/k_o$.

Thus, the opening and closing rates can be determined at each final temperature.

Monte Carlo Procedure. The dependence of the opening and closing times on the viscosity and changes in stability were modeled in terms of three parameters, as described in the Results and Discussion section. A simulated annealing procedure,[34,35] based on that introduced by Metropolis et al.,[36] was used. For each minimization procedure, random values for the parameters were picked from a plausible set of starting values. The minimization procedure was repeated for 50 independent sets of randomly chosen initial parameters.

Results and Discussion

Thermodynamics and Kinetics Measurements on Hairpin H. All measurements reported in this study are on hairpin H, which has the sequence 5′-CGGATAA(T_8)TTATCCG-3′. We have investigated in some detail the thermodynamics and kinetics of this hairpin.[15,16,29,37] In particular, the equilibrium melting profiles obtained as a function of oligomer concentration establish that this hairpin does not form a duplex under the conditions of our measurements. A related hairpin 5′-GGATAA-(T_4)TTATCC-3′, which was the subject of thermodynamic studies in the laboratory of Benight and co-workers,[38] was used as a model system for our T-jump spectrometer. For this hairpin, we showed, by substitution of a fluorescent nucleotide, 2-aminopurine (2AP), instead of A at each of the four available sites, that the thermodynamics and kinetics, as measured by fluorescence changes in 2AP, were identical to the thermodynamics and kinetics measured by absorbance changes at 266 nm. Thus, the local and global probes of the conformational state of the hairpin gave identical results and validated a two-state approximation to describe the thermodynamics and kinetics.[20,37] We also investigated the kinetics of hairpin H as a function of loop size and composition, with loop size varying from X_4 to X_{12} (X = A, T).[15,29,37] Near the melting temperatures, the characteristic time for forming hairpins scaled with the length L of the loop as $\sim L^2$, in close agreement with the predictions from polymer theory.[39] Thus, this hairpin is well-behaved and is suitable for further investigation of the viscosity dependence of the relaxation kinetics.

Effect of Glycerol on the Stability of Hairpins. Absorbance versus temperature melting profiles were obtained for the hairpin H, for five different glycerol concentrations: (i) 0%, (ii) 15%, (iii) 30%, (iv), 49%, and (v) 73% (w/w) glycerol, in 100 mM NaCl, pH 7.5 buffer. In addition, melting profiles for 49% and 74% glycerol were also obtained in high (1 M NaCl) salt conditions. The normalized melting profiles are shown in Figure 1. The melting temperature T_m, defined as the temperature at which the fraction $f_U = {}^1/_2$ decreases by more than 15 °C upon addition of ~50% glycerol and by nearly 30 °C upon addition of ~73% glycerol (inset of Figure 1). These data indicate a significant destabilizing effect of glycerol on hairpins and are consistent with a previous study on the effect of glycerol on dsDNA.[25] High salt conditions provide a means to compensate for the destabilizing effects of glycerol. For example, the T_m in ~50% glycerol, 1 M NaCl, is close to that in ~30% glycerol, 100 mM NaCl (~41and ~42 °C, respectively). Similarly, the T_m in ~75% glycerol, 1 M NaCl, is close to that in ~50% glycerol, 100 mM NaCl (~32 and ~36 °C, respectively).

Effect of Glycerol on the Kinetics of Hairpin Formation. The relaxation kinetics in response to a laser T-jump were measured for each glycerol sample over a temperature range around the T_m for each sample. Each kinetics curve was fitted to a single-exponential decay as described in the Methods section

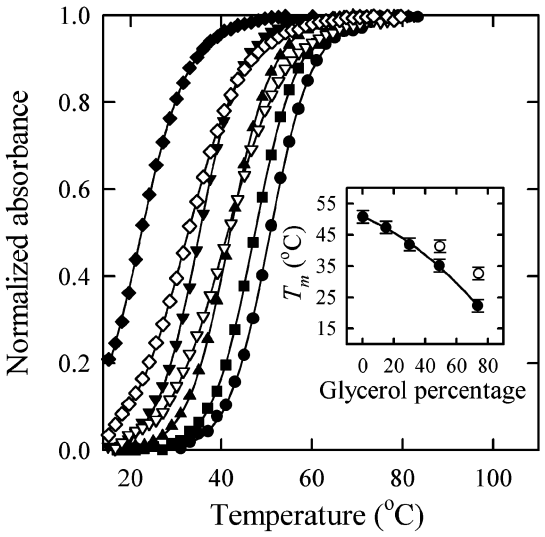

Figure 1. Melting profiles of hairpin H in solutions of varying glycerol−water mixtures. The normalized absorbance $[A(T) - A_L(T)]/[A_U(T) - A_L(T)]$ is plotted versus temperature for 0% (●), 15% (■), 30% (▲), 49% (▼), and 73% (◆), w/w, glycerol−water mixtures, in 100 mM NaCl, and 49% (▽) and 74% (◇), in 1 M NaCl. The continuous lines are a fit to the data, as described in the Methods section. Inset: The melting temperature T_m for each of the samples is plotted as a function of the corresponding percentage of glycerol in the sample in 100 mM NaCl (●) and in 1 M NaCl (○). The continuous line is drawn to guide the eye.

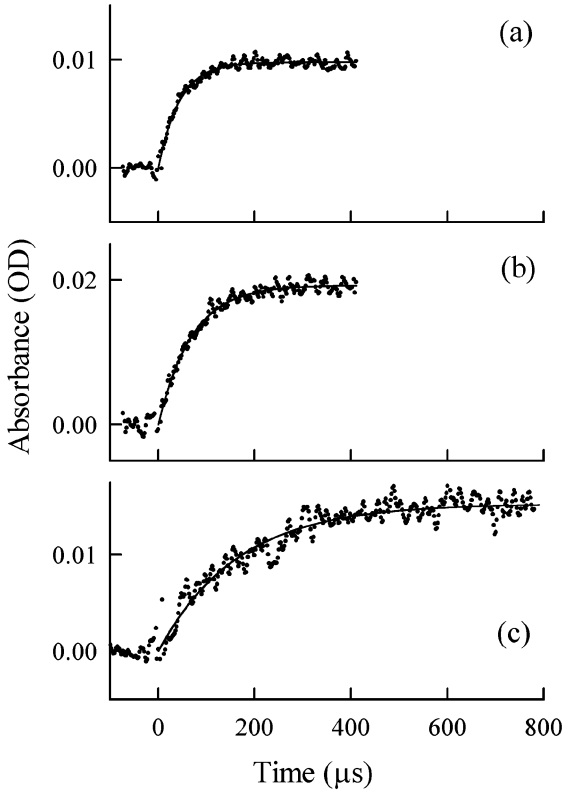

Figure 2. Relaxation kinetics for the hairpin H after a laser T-jump, for different glycerol samples in 100 mM NaCl, monitored by measuring the change in absorbance at 265 nm. The kinetics shown are for (a) 0% glycerol, with T-jump from 35.7 to 41.7 °C ($\tau_r = 44$ μs), (b) 30% glycerol, with T-jump from 35.5 to 42.1 °C ($\tau_r = 69$ μs), and (c) 50% glycerol, with T-jump from 33.1 to 37.0 °C ($\tau_r = 164$ μs).

(Figure 2). The relaxation times τ_r ($1/k_r$) thus obtained for all the glycerol samples are plotted versus the inverse of the final temperature (T_f) in Figure 3.

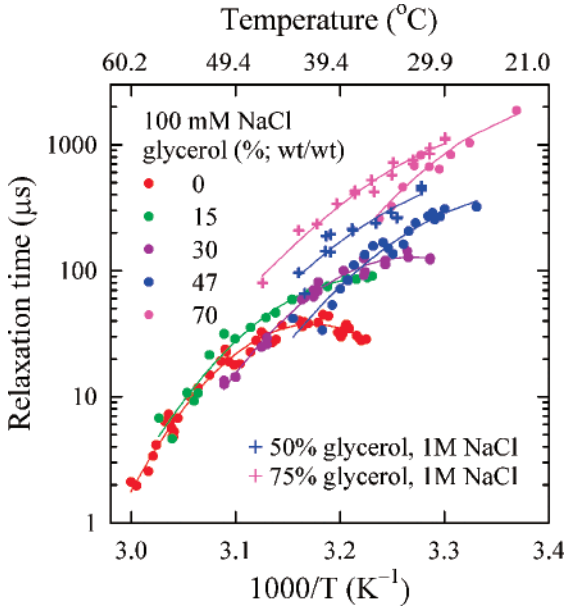

Figure 3. Relaxation times for the hairpin H in solutions of varying glycerol−water mixtures. The relaxation times τ_r, obtained from single-exponential fits to the relaxation kinetics after a laser T-jump, are plotted versus inverse temperature for different glycerol samples. The continuous lines are second-order polynomial fits to the data and are drawn to guide the eye.

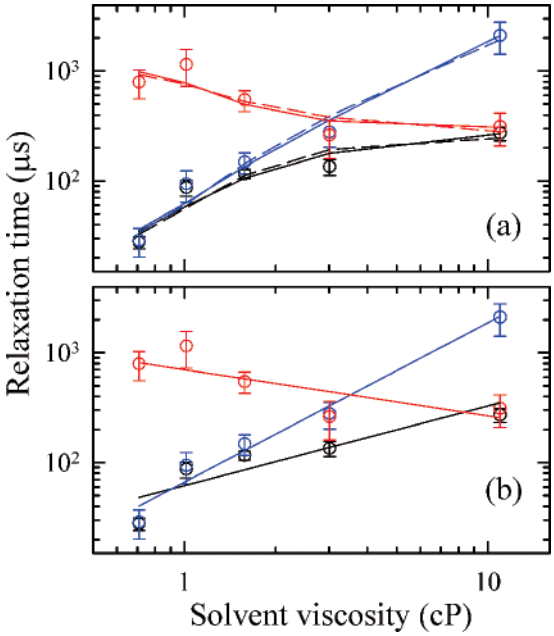

Figure 4. (a) Relaxation times and the opening and closing times at $T = 36$ °C for the different glycerol samples plotted versus the corresponding viscosity of the glycerol−water mixtures at that temperature. The relaxation times (black) are obtained from the data in 100 mM NaCl presented in Figure 3; the opening (red) and closing (blue) times are obtained as described in the Methods section. The continuous lines are a fit to the data using eq 4, with $\kappa = 0.97$ and $\alpha = 0.27$; the dashed lines are with $\kappa = 0.43$ and $\alpha = 0.55$. (b) The data are the same as in part a. The lines are linear fits on the double logarithmic plots with slopes of 0.72, −0.42, and 1.45 for τ_r, τ_o, and τ_c, respectively.

To investigate the dependence of the relaxation times and the opening and closing times on the glycerol concentration, the kinetics for the low salt (100 mM NaCl) samples were analyzed at a common reference temperature. The overlap in temperature between the different glycerol samples is limited because of the significant shift in T_m with increasing glycerol concentration. For example, the 0% glycerol samples were measured between 36.9 and 60.2 °C final temperatures, and the 70% glycerol samples were measured between 23.7 and 35.7 °C. We picked 36 °C as our reference temperature, to avoid long extrapolations for the 0% or 70% glycerol samples. The relaxation times and the opening and closing times, as a function of the solvent viscosity for each of the glycerol samples at 36 °C, are shown in Figure 4.

To interpret the viscosity dependence of the measured relaxation times, it is necessary to correct for the changes in stability at different glycerol concentrations. We make a simplifying assumption that an increase in the free energy of the hairpin (relative to the unfolded state) upon addition of glycerol ($\Delta\Delta G$) is reflected in a corresponding increase in the free energy of the transition state ($\alpha\Delta\Delta G$, with α between 0 and 1, Figure 5a). The hairpin closing (τ_c) and opening (τ_o) times were parametrized as

$$\tau_c(\eta) = \tau(\eta_0)\left(\frac{\eta}{\eta_0}\right)^{\kappa} \exp\left(\frac{\Delta G^{\ddagger}_{cw} + \alpha\Delta\Delta G}{RT}\right)$$

$$\tau_o(\eta) = \tau(\eta_0)\left(\frac{\eta}{\eta_0}\right)^{\kappa} \exp\left(\frac{\Delta G^{\ddagger}_{ow} + (\alpha - 1)\Delta\Delta G}{RT}\right) = \tau_c(\eta) \exp\left(-\frac{\Delta G_w + \Delta\Delta G}{RT}\right) \quad (3)$$

Here, $\tau(\eta_0)$ is a characteristic time that sets the time scale for the reaction in the absence of a barrier, at the reference temperature (with solvent viscosity η_0), κ describes the viscosity dependence of the opening and closing times, and $\Delta G^{\ddagger}_{cw}(\Delta G^{\ddagger}_{ow})$ is the free energy barrier for the closing (opening) step in water. The free energy difference between the fully intact hairpin and the unfolded state in water, $\Delta G_w = \Delta G^{\ddagger}_{cw} - \Delta G^{\ddagger}_{ow}$, and the corresponding free energy difference in each glycerol concentration, $\Delta G_g = \Delta G_w + \Delta\Delta G$, is calculated from the equilibrium constant, obtained from the melting profiles, at the reference temperature T.

Since the relaxation times in Figure 4 are at a single temperature, there is no independent information about $\tau(\eta_0)$ and $\Delta G^{\ddagger}_{cw}$ in this data set. The opening and closing times at a single temperature were therefore written in terms of three free parameters, κ, α, and a preexponential $\lambda(\eta_0,T) = \tau(\eta_0) \exp(\Delta G^{\ddagger}_{cw}/RT)$, as follows

$$\tau_c(\eta) = \lambda(\eta_0,T)\left(\frac{\eta}{\eta_0}\right)^{\kappa} \exp\left(\frac{\alpha\Delta\Delta G}{RT}\right)$$

$$\tau_o(\eta) = \tau_c(\eta) \exp\left(-\frac{\Delta G_w + \Delta\Delta G}{RT}\right) \quad (4)$$

The residuals between the data and the fit were minimized using a Monte Carlo procedure, as described in the Methods section. The results of this analysis are shown in Figure 4a. We find that the apparent viscosity dependence of τ_c and τ_o can be described equally well by assigning nearly all the changes in τ_c and τ_o to a change in solvent viscosity ($\kappa \approx 1$) and a small change in the stability of the transition state relative to the unfolded state ($\alpha \approx 0.3$) or by a weaker viscosity dependence ($\kappa \approx 0.4$) and a larger change in the stability of the transition state ($\alpha \approx 0.6$). Thus, this analysis is, at best, ambiguous in interpreting the viscosity dependence of the opening and closing times.

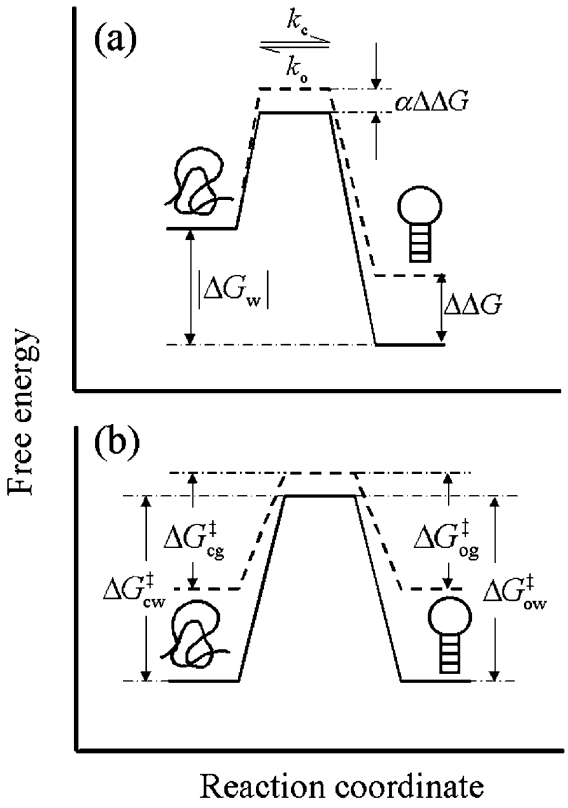

Figure 5. Schematic representation of the free energy versus an effective reaction coordinate for hairpin formation in water (continuous line) and in a glycerol−water mixture (dashed line). (a) Free energy profiles at a fixed temperature. A linear free energy approximation is assumed in which the transition state is destabilized by some fractional amount ($\alpha\Delta\Delta G$) when the hairpin state is destabilized by an amount $\Delta\Delta G$. (b) Free energy profiles at the corresponding melting temperatures ($T = T_w$ in water, and $T = T_g$ in glycerol−water mixture, with $T_g < T_w$).

We can now compare our experimental results and analysis with those of Klenerman and co-workers who monitored the conformational fluctuations of the fluorescently labeled ssDNA hairpin, 5′-GGGAA(A_{30})TTCCC-3′, using fluorescence correlation spectroscopy.[24] They monitored the decay of a fluorescence correlation function, which they modeled as a stretched exponential of the form $\exp[-(t/\tau_r)^{\beta}]$. They measured the relaxation time τ_r at 20 °C for increasing glycerol concentrations up to 55% (w/w) glycerol and found that τ_r scales with viscosity as $\eta^{0.83}$. If we repeat the analysis of Klenerman and co-workers and fit the viscosity dependence of our observed relaxation times τ_r, then we obtain an apparent exponent $\kappa_{app} \approx 0.72$ (Figure 4b), in close agreement with the apparent exponent of 0.83 reported by Klenerman and co-workers. However, as pointed out earlier, this analysis does not take into account the destabilizing effect of glycerol and gives erroneous viscosity dependencies, $\tau_o \sim \eta^{-0.42}$ and $\tau_c \sim \eta^{1.45}$, with different values (and opposite signs) of the apparent scaling exponents for the opening and closing times (Figure 4b).

Isostability Conditions Obtained with Varying Glycerol and Temperature. It is clear from the analysis presented in the previous section that it is necessary to separate the effect of the viscogenic cosolvent on stability from that on the viscosity. Previous attempts at investigating the viscosity dependence of the protein folding kinetics have relied on isostability measurements. In the case of proteins, addition of viscogenic cosolvents such as glycerol or ethylene glycol have a stabilizing effect, which can be compensated for by the destabilizing effects of a denaturing agent like urea or guanidine hydrochloride. These isostability studies assume that the viscogenic cosolvent and the denaturant compensate to the same degree in the transition state as in the folded state relative to the unfolded state. Several such studies reveal a linear relation between the folding times and the solvent viscosity.[26−28]

TABLE 1: Temperature and Viscosity Values for Isostability Conditions

glycerol (%, w/w)	$f_U = 0.3$		$f_U = 0.5$		$f_U = 0.7$	
	T (°C)	η (cP)	T (°C)	η (cP)	T (°C)	η (cP)
0[a]	46.8	0.58	50.8	0.54	54.8	0.51
15[a]	43.5	0.87	47.4	0.81	51.5	0.75
30[a]	38.1	1.5	42.0	1.37	46.1	1.25
47[a]	31.8	3.42	35.9	3.02	40.1	2.68
70[a]	19.0	23.62	23.8	18.75	29.0	14.74
50[b]	35.7	3.47	41.2	2.96	46.8	2.54
75[b]	27.2	23.49	32.4	18.32	37.7	14.51

[a] In 100 mM NaCl. [b] In 1 M NaCl.

Here, we take a very simple approach to reanalyze the viscosity dependence of the folding of hairpins under isostability conditions by using temperature as the additional parameter to compensate for the destabilizing effect of glycerol. For each of the glycerol samples, we determine, from the melting profiles, the temperature corresponding to a fixed value of the equilibrium constant and obtain the opening and closing times for each glycerol−water sample at that temperature. For example, the temperatures at which each of the samples have an equilibrium constant, $K_{eq} = 1$, are the T_m for each sample. Table 1 summarizes the temperatures and viscosities, for each of the samples, at which the equilibrium constants (unfolded fractions) are (i) $K_{eq} = 2.33$ ($f_U = 0.3$), (ii) $K_{eq} = 1$ ($f_U = 0.5$), and (iii) $K_{eq} = 0.43$ ($f_U = 0.7$). The dependencies of the opening and closing times on the solvent viscosity are plotted in a double logarithmic plot in Figure 6.

Although the data shown in Figure 6 consist of measurements at different temperatures, the effect of temperature on the rate constants is assumed not to perturb the results significantly. This assumption is rationalized as follows. Constraining the equilibrium constant for all samples to be identical implies that $\Delta G_w/RT_w = \Delta G_g/RT_g$, where T_w and T_g are the temperatures in water and in a glycerol−water mixture, respectively, that correspond to identical equilibrium constants. It therefore follows that

$$\frac{\Delta G^{\ddagger}_{cw}}{RT_w} - \frac{\Delta G^{\ddagger}_{ow}}{RT_w} = \frac{\Delta G^{\ddagger}_{cg}}{RT_g} - \frac{\Delta G^{\ddagger}_{og}}{RT_g} \qquad (5)$$

where $\Delta G^{\ddagger}_{cg}(\Delta G^{\ddagger}_{og})$ is the free energy barrier for the closing (opening) step in the glycerol−water mixture at temperature T_g. The effect of these isostability conditions on the measured rates is best visualized in terms of the free energy schematic for water and glycerol−water mixture at their respective melting temperatures (Figure 5b). The hairpin state in glycerol has a higher free energy than that in water, because of the destabilizing effects of glycerol. Under our isostability conditions, for which $T_g < T_w$, the unfolded state in glycerol also has a higher free energy than that in water (from entropic considerations). The free energy barrier, which is primarily entropic for the closing step, is lower in glycerol than in water (again, because $T_g < T_w$). The effect on the rates from the difference in barrier heights in glycerol and in water is compensated for by the effect on the rates from the temperature dependence in the Boltzmann factor, and this compensation is exact if we equate each term in eq 5, such that $\Delta G^{\ddagger}_{cw}/RT_w = \Delta G^{\ddagger}_{cg}/RT_g$ and $\Delta G^{\ddagger}_{ow}/RT_w = \Delta G^{\ddagger}_{og}/RT_g$.

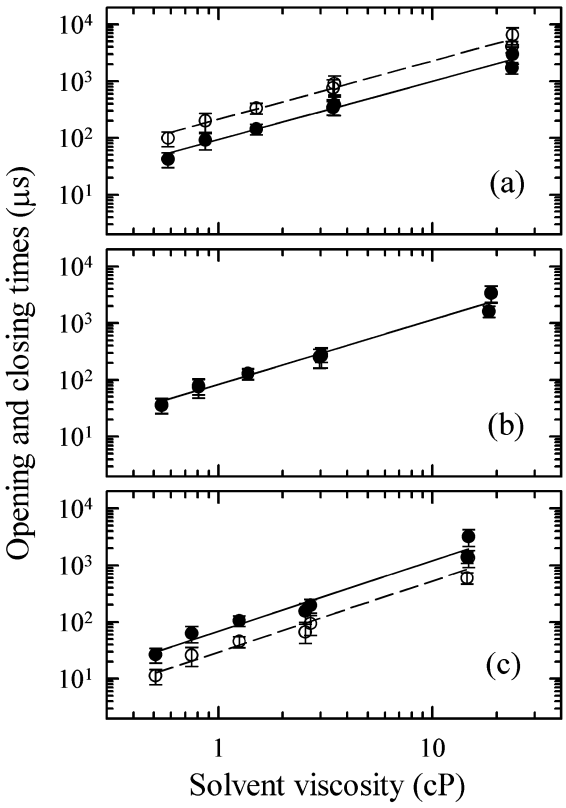

Figure 6. Isostability plots of opening and closing times in solutions of varying glycerol−water mixtures. The opening (○) and closing (●) times, obtained from the data presented in Figure 3, are plotted as a function of the solvent viscosity for each glycerol−water mixture and for both 100 mM and 1 M NaCl, for temperatures at which the fraction of unfolded molecules f_U is (a) 0.3, (b) 0.5, and (c) 0.7. The continuous lines are linear fits on the double logarithmic plots with slopes for the opening and closing times, respectively, of (a) 0.99 and 0.99, (b) 1.09 and 1.09, and (c) 1.19 and 1.20.

The only temperature dependence that remains in the time constants is in the preexponential factor, which, according to Kramer's theory in the diffusive limit, scales with temperature as k_BT/D, where k_B is Boltzmann's constant and D is a characteristic diffusion coefficient for motion along the reaction coordinate.[40−42] The viscosity dependence of D is explicitly included in the preexponential factor as $(\eta/\eta_0)^\kappa$ (see eq 3). Therefore, the characteristic time $\tau(\eta_0)$ is only weakly dependent on temperature and, to first approximation, is assumed to be independent of temperature.

The slopes of linear fits to the $\log(\tau)$ versus $\log(\eta)$ data yield a value of $\kappa = 1.1 \pm 0.1$. Note that the measurements done in ∼50% and ∼75% glycerol, in 1 M NaCl, also fall on this linear plot (Figure 6), thus lending further support to the isostability approach presented here. An increase in salt concentration from 100 mM to 1 M NaCl has a significant effect on the stability of the hairpin, comparable to a change in glycerol concentration from, e.g., 30% to 50% (Figure 1), but the effect on solution viscosity is negligible. The data points on the isostability plots from the two sets of salt conditions in ∼50% glycerol are within the error in these measurements. The slightly larger noise in the ∼70−75% glycerol samples is most likely from the uncertainty in the determination of the equilibrium constant and hence the opening and closing times, at these high glycerol concentrations, for which the lower baselines in the absorbance melting profiles are not very well determined (Figure 1).

We can now return to the question posed in the Introduction: Why is hairpin formation so slow? This question is opposite to the one posed in connection with the folding of proteins by Levinthal,[43] frequently referred to as the Levinthal paradox; he argued that it should take longer than the age of the universe for proteins to fold if they randomly sampled all conformational space. Thus, the question underlying the field of protein folding became: Why do proteins fold so fast?[44] The resolution of this paradox comes from the realization that in proteins there is a strong bias toward the native state, leading to a "funnel-shaped" free energy surface, with an ensemble of structures in the transition state and a pronounced global minimum.[45−48]

Several theoretical and computational studies of protein folding suggest that the folding funnel is not smooth but has a "roughness" as a result of intrachain interactions, especially under folding conditions, which decreases the effective configurational diffusion coefficient by a factor of $\sim\exp[-(\epsilon/RT)^2]$, where ϵ is the amplitude of the roughness.[49−51] Even for a polypeptide chain designed not to have any secondary structure, measurements of the first contact time between the two ends suggest an ∼16-fold decrease in the effective diffusion coefficient arising from transient intrachain interactions.[52]

In the case of ss oligomers, a random sampling of all conformational states in the unfolded state, assuming an ideal semiflexible polymer, leads to an estimate for the end-to-end contact time of tens of nanoseconds for an ∼10-nucleotide-long chain. There is mounting experimental evidence suggesting that intrachain interactions in ssDNA that lead to nonideal behavior are nonnegligible. Force extension measurements that monitor the elastic response of a biopolymer show significant deviations from a semiflexible polymer description for ssDNA for both high and low ionic conditions, especially in the limit of low (<10 pN) forces.[53−55] The low force behavior under high ionic solutions has been explained by various theoretical models as arising from secondary structures (hairpins) that form as a result of base-pairing interactions along a ssDNA.[56−59] The behavior at low ionic conditions has been explained as arising from the increased charge and hence the increased electrostatic repulsion of the ssDNA segments, resulting in an increase in the effective statistical segment length of the chain.[58,59]

Another measure of the semiflexible polymer nature of ssDNA comes from the dependence of loop-closure probability on the length of the loop. The simplest description of loop closure, which takes into account the entropic cost for loop formation, suggests that the closing time should scale as $\tau_c \sim L^2$, where L is the length of the loop, and that the stabilizing free energy of the hairpin should increase with decreasing loop size as $\sim 2RT \ln(L)$, for loop sizes $L \geq 10$.[60] However, although the kinetics of the closing step show the expected scaling behavior, the dependence of the melting temperature of the hairpins on the loop size show that the hairpin stability deviates quite significantly from this simple description and varies as $\sim\alpha RT \ln(L)$ where $\alpha \approx 7$ for loops ranging from 4 to 12 bases and $\alpha \approx 3-5$ for loops ranging from 10 to 30 bases.[15,37] Therefore, smaller loops are much more stable than expected from entropy considerations alone, presumably from favorable stacking interactions within the loop and exclusion of water in tighter loops.[61]

Thus, one may ask whether the slow times observed for the folding of hairpins are because these intrachain interactions in the unfolded state lead to a roughness in the energy landscape that impedes the chain dynamics prior to the formation of the critical nucleus.[20,29] This slowing down could arise from (i)

nonnative base pairs that do not lead to a complete hairpin and that act as dead ends during the folding process or (ii) nonnative stacking interactions (misstacked bases).[29,62] In a series of papers, we had proposed a configurational diffusion model that suggested that the hairpin gets trapped in misfolded states, leading to a decrease in the effective diffusion coefficient for the chain dynamics and hence an increase in the nucleation time.[16,20,29] The model does not require that the traps be stable; it is sufficient that they introduce a roughness in the free energy surface. A characteristic roughness of $\epsilon \approx 1.5$ kcal/mol would be enough to decrease the effective diffusion coefficient and increase the nucleation time by $\sim 600\times$ at 25 °C. Large-scale, parallel, molecular dynamics simulations of Pande and co-workers on an all-atom model of a RNA hairpin 5′-GGGC-[GCAA]GCCU-3′ support the notion that misfolded states, with mismatched base pairs or intrastrand stracking interactions, act as transient traps in the collapse and folding of this small hairpin.[62]

The two missing pieces of the configurational diffusion model were the viscosity dependence and a direct measurement of the end-to-end contact times. A nearly linear scaling of the opening and closing times with solvent viscosity observed for hairpin formation, once the changes in stability upon addition of viscogenic solvents are appropriately compensated for, indicate that the rate-determining steps in the formation of hairpins involve diffusion of the polynucleotide chain through the solvent. Recently, the first set of measurements for the end-to-end contact time for short oligomers have been reported.[63] The measurements yield surprisingly slow contact times of $\sim$400 ns for a four-nucleotide poly(dT) strand and ~ 8 μs for a four-nucleotide poly(dA) strand, suggesting that either the effective stiffness of these chains is much higher than previous estimates[64−66] or that intrachain interactions do indeed impede the dynamics.

In our analysis of the viscosity dependence under isostability conditions, we did not explicitly include the contribution to the preexponential from the roughness in the free energy, the amplitude of which is clearly dependent on both the temperature and the amount of glycerol in the sample. An increase in temperature or an increase in glycerol concentration is expected to decrease the roughness, by destabilizing the transient misfolded conformations relative to the unfolded state. However, since our isostability conditions are such that measurements in glycerol are at a lower temperature ($T_g < T_w$), we can assume, to first approximation, that $\epsilon_w/RT_w \approx \epsilon_g/RT_g$, where ϵ_w (ϵ_g) is the characteristic roughness in water (glycerol−water mixture). Thus, the contribution to the configurational diffusion coefficient from the roughness is approximately the same under isostability conditions for varying glycerol concentrations. Our observed linear scaling of the opening/closing times with solvent viscosity, which gives identical results under low and high salt conditions, provides further support for the assumption that the change in roughness with change in solvent condition is not a significant factor.

Note that a linear dependence of the time constants with viscosity does not prove that the kinetics are not reaction-controlled; Kramer's theory points out that any barrier crossing is limited by friction over the barrier and if this friction is dominated by solvent damping, then the reaction will exhibit viscosity dependence.[40,41] However, the lack of a significant activation enthalpy for the closing step, together with the slow end-to-end contact formation observed experimentally, supports our conclusion that configurational diffusion of the polynucleotide, impeded by significant intrachain interactions, sets the time scale of several microseconds for hairpin formation.

Marko and co-workers have suggested an alternative explanation for the slow times for hairpin formation.[67] In their study, they apply the kinetic zipper model to simulate the opening and closing of a RNA hairpin that is held at a constant force of a few piconewtons to simulate the force-induced unfolding measurements of Bustamante and co-workers.[68] The values of the parameters in their model that best describe the experiments suggest that, in the absence of applied force, the time required to close each base pair would be $\sim$300 ns, which gives closing times of ~ 3 μs for a hairpin with $\sim$10 bases in the stem. Thus, in their model, the slow times for hairpin formation are not from the slow nucleation step but rather from the slow zipping of the stem by the successive closing of base pairs. Their model makes a prediction that the closing times should scale linearly with the length of the stem. These predictions have yet to be tested in a systematic way for ssDNA or RNA hairpins.

Finally, our results that the opening and closing times scale nearly linearly with the solvent viscosity do not contradict the notion that "internal friction", arising from intrachain interactions, plays a significant role in the rate-determining step. Hagen and co-workers[28,69] have shown that small proteins that fold on time scales of several microseconds exhibit folding times (τ_f) that extrapolate to finite value in the limit of zero solvent viscosity, i.e., $\tau_f \approx \tau_s + \tau_{int}$, with τ_s scaling linearly with solvent viscosity and τ_{int} controlled by internal friction and insensitive to solvent viscosity. Our data at the present time do not sample enough points at low solvent viscosities to draw any conclusions about the limiting values of the opening and closing times.

Conclusions

We report here the first study on the viscosity dependence of hairpin dynamics, after correcting for the inevitable and quite significant changes in the stability of the hairpin from the addition of viscogenic agents. The conditions for isostability are obtained by varying the temperature and/or salt concentration to compensate for the destabilizing effect of glycerol. Our results that both the opening and the closing times for hairpin formation scale nearly linearly with the solvent viscosity provide a self-consistent validation of this approach. The observed viscosity dependence indicates that diffusion of the polynucleotide chain through the solvent plays a role in the rate-determining step for hairpin formation and is consistent with the notion that configurational diffusion slowed by transient trapping in misfolded states sets the time scale of hairpin formation. This conclusion is supported by two additional studies. One is the computational study of the folding of a RNA hairpin by Pande and co-workers, in which the initial collapse and reorganization of intrastrand contacts, with an observed collapse time of ~ 8 μs, is postulated to be the rate-determining step in hairpin formation.[62] The second is the very slow first contact time between the two ends of a ss oligomer, reported by Wang and Nau.[63]

Acknowledgment. We thank John Marko for many helpful discussions. We also thank Albert S. Benight for the generous use of his absorption spectrometer. This work was supported by the National Science Foundation through grants MCB-9722295 and MCB-0211254.

References and Notes

(1) Dai, X.; Greizerstein, M. B.; Nadas-Chinni, K.; Rothman-Denes, L. B. *Proc. Natl. Acad. Sci. U.S.A.* **1997**, *94*, 2174.

(2) Lilley, D. M. *Nucleic Acids Res.* **1981**, *9*, 1271.
(3) Roth, D. B.; Menetski, J. P.; Nakajima, P. B.; Bosma, M. J.; Gellert, M. *Cell* **1992**, *70*, 983.
(4) Tang, J. Y.; Temsamani, J.; Agrawal, S. *Nucleic Acids Res.* **1993**, *21*, 2729.
(5) Bonnet, G.; Tyagi, S.; Libchaber, A.; Kramer, F. R. *Proc. Natl. Acad. Sci. U.S.A.* **1999**, *96*, 6171.
(6) Varani, G. *Annu. Rev. Biophys. Biomol. Struct.* **1995**, *24*, 379.
(7) Uhlenbeck, O. C. *Nature* **1990**, *346*, 613.
(8) Marino, J. P.; Gregorian, R. S.; Csankovszki, G.; Crothers, D. M. *Science* **1995**, *268*, 1448.
(9) Draper, D. E. *J. Mol. Biol.* **1999**, *293*, 255.
(10) Rupert, P. B.; Massey, A. P.; Sigurdsson, S. T.; Ferre-D'Amare, A. R. *Science* **2002**, *298*, 1421.
(11) Lilley, D. M. *Trends Biochem. Sci.* **2003**, *28*, 495.
(12) Cech, T. R.; Zaug, A. J.; Grabowski, P. J. *Cell* **1981**, *27*, 487.
(13) Thirumalai, D.; Woodson, S. A. *Acc. Chem. Res.* **1996**, *29*, 433.
(14) Cantor, C. R.; Schimmel, P. R. *The Behavior of Biological Macromolecules*; W. H. Freeman and Company: New York, 1980.
(15) Shen, Y.; Kuznetsov, S. V.; Ansari, A. *J. Phys. Chem. B.* **2001**, *105*, 12202.
(16) Ansari, A.; Kuznetsov, S. V. Hairpin Formation in Polynucleotides: A Simple Folding Problem? In *Biological Nanostructures and Applications of Nanostructures in Biology: Electrical, Mechanical and Optical Properties*; Stroscio, M. A., Dutta, M., Eds.; Kluwer Academic Publishers: New York, 2004.
(17) Gralla, J.; Crothers, D. M. *J. Mol. Biol.* **1973**, *73*, 497.
(18) Porschke, D. *Biophys. Chem.* **1974**, *1*, 381.
(19) Bonnet, G.; Krichevsky, O.; Libchaber, A. *Proc. Natl. Acad. Sci. U.S.A.* **1998**, *95*, 8602.
(20) Ansari, A.; Kuznetsov, S. V.; Shen, Y. *Proc. Natl. Acad. Sci. U.S.A.* **2001**, *98*, 7771.
(21) Wang, J. C.; Davidson, N. *J. Mol. Biol.* **1966**, *19*, 469.
(22) Wang, J. C.; Davidson, N. *J. Mol. Biol.* **1966**, *15*, 111.
(23) Wang, J. C.; Davidson, N. *Cold Spring Harbor Symp. Quant. Biol.* **1968**, *33*, 409.
(24) Wallace, M. I.; Ying, L.; Balasubramanian, S.; Klenerman, D. *Proc. Natl. Acad. Sci. U.S.A.* **2001**, *98*, 5584.
(25) Bonner, G.; Klibanov, A. M. *Biotechnol. Bioeng.***2000**, *68*, 339.
(26) Jacob, M.; Schindler, T.; Balbach, J.; Schmid, F. X. *Proc. Natl. Acad. Sci. U.S.A.* **1997**, *94*, 5622.
(27) Plaxco, K. W.; Baker, D. *Proc. Natl. Acad. Sci. U.S.A.* **1998**, *95*, 13591.
(28) Qiu, L.; Hagen, S. J. *J. Am. Chem. Soc.* **2004**, *126*, 3398.
(29) Ansari, A.; Shen, Y.; Kuznetsov, S. V. *Phys. Rev. Lett.* **2002**, *88*, 069801.
(30) Newman, A. A. *Glycerol*; CRC Press: Cleveland, OH, 1968.
(31) Chalikian, T. V.; Volker, J.; Plum, G. E.; Breslauer, K. J. *Proc. Natl. Acad. Sci. U.S.A.* **1999**, *96*, 7853.
(32) Rouzina, I.; Bloomfield, V. A. *Biophys. J.* **1999**, *77*, 3242.
(33) Hofrichter, J. Laser Temperature-Jump Methods for Studying Folding Dynamics. In *Protein Structure, Stability, and Folding*; Murphy, K. P., Ed.; Methods in Molecular Biology 168; Humana Press: Totowa, NJ, 2001.
(34) Kirkpatrick, S.; Gelatt, C. D.; Vecchi, M. P. *Science* **1983**, *220*, 671.
(35) Press, W. H.; Flannery, B. P.; Teukolsky, S. A. *Numerical Recipes: The Art of Scientific Computing*; Cambridge University Press: Cambridge, U. K., 1986.
(36) Metropolis, N.; Rosenbluth, A. W.; Rosenbluth, M. N.; Teller, A. H.; Teller, E. *J. Chem. Phys.* **1953**, *21*, 1087.
(37) Kuznetsov, S. V.; Shen, Y.; Benight, A. S.; Ansari, A. *Biophys. J.* **2001**, *81*, 2864.
(38) Vallone, P. M.; Paner, T. M.; Hilario, J.; Lane, M. J.; Faldasz, B. D.; Benight, A. S. *Biopolymers* **1999**, *50*, 425.
(39) DeGennes, P. G. *Scaling Concepts in Polymer Physics*; Cornell University Press: Ithaca, NY, 1979.
(40) Kramers, H. A. *Physica* **1940**, *7*, 284.
(41) Hanggi, P.; Talkner, P.; Borkovec, M. *Rev. Mod. Phys.* **1990**, *62*, 251.
(42) Schuler, B.; Lipman, E. A.; Eaton, W. A. *Nature* **2002**, *419*, 743.
(43) Levinthal, C. How to Fold Graciously? In *Mossbauer Spectroscopy in Biological Systems*, Proceedings of a Meeting held at Allerton House, Monticello, IL; Debrunner, P., Tsibris, J. C. M., Münck, E., Eds.; University of Illinois Press: Urbana, IL, 1969.
(44) Baldwin, R. L. *Proc. Natl. Acad. Sci. U.S.A.* **1996**, *93*, 2627.
(45) Zwanzig, R.; Szabo, A.; Bagchi, B. *Proc. Natl. Acad. Sci. U.S.A.* **1992**, *89*, 20.
(46) Leopold, P. E.; Montal, M.; Onuchic, J. N. *Proc. Natl. Acad. Sci. U.S.A.* **1992**, *89*, 8721.
(47) Sali, A.; Shakhnovich, E.; Karplus, M. *Nature* **1994**, *369*, 248.
(48) Onuchic, J. N.; Wolynes, P. G.; Luthey-Schulten, Z.; Socci, N. D. *Proc. Natl. Acad. Sci. U.S.A.* **1995**, *92*, 3626.
(49) Zwanzig, R. *Proc. Natl. Acad. Sci. U.S.A.* **1988**, *85*, 2029.
(50) Bryngelson, J. D.; Wolynes, P. G. *J. Phys. Chem.* **1989**, *93*, 6902.
(51) Socci, N. D.; Onuchic, J. N.; Wolynes, P. G. *J. Chem. Phys.* **1996**, *104*, 5860.
(52) Lapidus, L. J.; Eaton, W. A.; Hofrichter, J. *Proc. Natl. Acad. Sci. U.S.A.* **2000**, *97*, 7220.
(53) Bustamante, C.; Smith, S. B.; Liphardt, J.; Smith, D. *Curr. Opin. Struct. Biol.* **2000**, *10*, 279.
(54) Maier, B.; Bensimon, D.; Croquette, V. *Proc. Natl. Acad. Sci. U.S.A.* **2000**, *97*, 12002.
(55) Wuite, G. J.; Smith, S. B.; Young, M.; Keller, D.; Bustamante, C. *Nature* **2000**, *404*, 103.
(56) Gerland, U.; Bundschuh, R.; Hwa, T. *Biophys. J.* **2001**, *81*, 1324.
(57) Montanari, A.; Mezard, M. *Phys. Rev. Lett.* **2001**, *86*, 2178.
(58) Zhang, Y.; Zhou, H.; Ou-Yang, Z. C. *Biophys. J.* **2001**, *81*, 1133.
(59) Cocco, S.; Marko, J. F.; Monasson, R.; Sarkar, A.; Yan, J. *Eur. Phys. J. E* **2003**, *10*, 249.
(60) Mathews, D. H.; Sabina, J.; Zuker, M.; Turner, D. H. *J. Mol. Biol.* **1999**, *288*, 911.
(61) Vallone, P. M.; Benight, A. S. *Nucleic Acids Res.* **1999**, *27*, 3589.
(62) Sorin, E. J.; Rhee, Y. M.; Nakatani, B. J.; Pande, V. S. *Biophys. J.* **2003**, *85*, 790.
(63) Wang, X.; Nau, W. M. *J. Am. Chem. Soc.* **2004**, *126*, 808.
(64) Mills, J. B.; Vacano, E.; Hagerman, P. J. *J. Mol. Biol.* **1999**, *285*, 245.
(65) Tinland, B.; Pluen, A.; Sturm, J.; Weill, G. *Macromolecules* **1997**, *30*, 5763.
(66) Smith, S. B.; Cui, Y.; Bustamante, C. *Science* **1996**, *271*, 795.
(67) Cocco, S.; Marko, J. F.; Monasson, R. *Eur. Phys. J. E* **2003**, *10*, 153.
(68) Liphardt, J.; Onoa, B.; Smith, S. B.; Tinoco, I. J.; Bustamante, C. *Science* **2001**, *292*, 733.
(69) Pabit, S. A.; Roder, H.; Hagen, S. J. *Biochemistry* **2004**, *43*, 12532.